

Evidence for Spin-Spin Effects in \vec{p}^- - ^{13}C Elastic Scattering

B. v. Przewoski, P. D. Eversheim, F. Hinterberger, and U. Lahr

Institut für Strahlen- und Kernphysik der Universität Bonn, Nussballe 14-16, D-5300 Bonn, West Germany

J. Campbell,^(a) J. Götz, M. Hammans, R. Henneck, G. Masson, and I. Sick

Institut für Physik der Universität Basel, Klingelbergstrasse 82, CH-4056 Basel, Switzerland

W. Bauhoff

Institut für Theoretische Kernphysik der Universität Hamburg, Luruper Chaussee 149, D-2000 Hamburg, West Germany

(Received 13 November 1989)

The depolarization parameter D in proton- ^{13}C elastic scattering at 72 MeV has been measured with an accuracy of 0.003–0.004 per data point. D was found to deviate from unity by ~ 0.02 around 65° , which is unambiguous evidence for a nucleon-nucleus spin-spin interaction. The data are well described by a microscopic calculation as well as by a phenomenological optical-model potential, which includes a real spherical spin-spin potential of strength $V_{ss} = 0.7 \pm 0.1$ MeV.

PACS numbers: 24.70.+s, 24.10.Ht, 25.40.Cm, 27.20.+n

A complete description of the nucleon-nucleus interaction has to take into account effects due to the coupling of projectile spin and target spin (for a review, see Ref. 1). These effects are large and well known in the underlying NN interaction due to the spin-spin and tensor force between two nucleons. For nucleon-nucleus scattering one expects greatly reduced spin-flip probabilities mainly because spin flip occurs only in the interaction with a valence nucleon, and not with the many nucleons of an inert core. However, this simple picture can be drastically modified by core polarization effects.

Various experimental approaches have been used to demonstrate the presence of spin-spin effects:¹ (1) transmission experiments of polarized neutrons through polarized targets;^{1,2} (2) analysis of (n, γ) slow-neutron-capture data;³ and (3) measurements of the depolarization parameter $D(\theta)$ for elastic proton scattering.^{1,4} The interpretation of these data was contested subsequently^{1,5,6} due to the presence of contributions from sources other than the spin-spin interaction. The most dominant among these are compound-nucleus effects at energies below 30 MeV and “quadrupole spin flip” or “nuclear reorientation” effects that occur in the interaction with targets of spin $> \frac{1}{2}$. The only experiment without these deficiencies⁷ did not reach a significant level of accuracy. The question of spin-spin potentials is therefore still an open one, with predictions for the strength of this potential ranging from 0 to 2 MeV.¹⁻³ The present Letter reports the first unambiguous determination of the spin-spin interaction via a measurement of $D(\theta)$ for elastic scattering from a spin- $\frac{1}{2}$ nucleus at an energy where compound-nucleus effects are negligible.

The principle of the experiment is based on double scattering of polarized spin- $\frac{1}{2}$ particles from a spin- $\frac{1}{2}$ target. The depolarization parameter D is given by the

relationship⁸

$$D = \frac{p_1^\pm (1 + A_1 p_0^\pm) - A_1}{p_0^\pm}, \quad (1)$$

which connects the incident beam polarization p_0^\pm , the analyzing power A_1 in the scattering, the scattered beam polarization p_1^\pm , and D (see Fig. 1). Superscripts refer to the sign of the incident beam polarization, the direction of which is the y direction, i.e., normal to the scattering plane.

The experiment was performed at the Paul Scherrer Institut (PSI) injector cyclotron. The setup (see Fig. 1 and Ref. 9 for more detail) consisted of three major

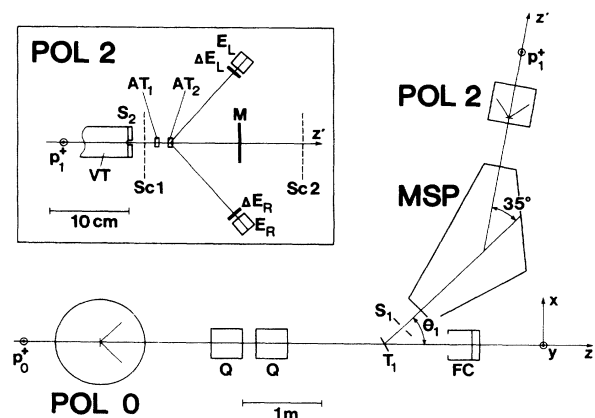


FIG. 1. Schematic layout of the experiment, showing the polarimeters (POL0, POL2), the target (T_1), the Faraday cup (FC), and the magnetic spectrometer (MSP). Inset: POL2 shown in more detail; the MSP beam tube (VT) with the exit slits (S_2), the active targets (AT_1, AT_2), and the side telescopes ($\Delta E_L - E_L, \Delta E_R - E_R$). Intensity profiles were measured along the dashed lines, denoted by Sc1 and Sc2.

components: the polarimeter POL0 to measure the incident beam polarization p_0^\pm , the magnetic spectrometer MSP to select elastically scattered protons, and the polarimeter POL2 to measure the scattered beam polarization p_1^\pm . The beam polarimeter POL0 contained two NaI(Tl) detectors at $\pm 44.0^\circ$ which measured the left-right asymmetries ϵ_0^\pm in the scattering from natural carbon. The target foils (100–400 $\mu\text{g}/\text{cm}^2$) were always kept in the beam, thus providing a continuous sampling of the beam polarization. Intensity profiles, measured periodically upstream and downstream of POL0, showed that the beam axis was aligned with the nominal axis to within 0.5 mm and 3 mrad. After passing through POL0 the beam was refocused onto the scattering target (T_1). The beam position on target was measured continuously by a secondary-electron-emission monitor and stabilized via feedback to steering magnets. The ^{13}C targets (100–200 mg/cm^2) were prepared from enriched ^{13}C , while the natural carbon targets (90 mg/cm^2), used for normalization, were cut from high-purity graphite.¹⁰ The beam was stopped in a shielded Faraday cup (FC) equipped with electron suppression. The spectrometer, of type QQDQQ, focused elastically scattered protons from T_1 onto the two active plastic-scintillator targets (AT₁, AT₂, each 5 mm thick) of POL2. The energy signals from either AT were gain matched to the energy signals of the NaI(Tl) side detectors. Requiring coincidences between one of the active targets, a side detector, and an additional ΔE plastic detector in front of the side detector provided good background suppression. The time of flight between all detectors was also recorded.

The whole POL2 setup was adjustable in the horizontal plane and could be rotated ($0^\circ \leq \phi_2 \leq 180^\circ$) around the direction of the scattered beam (i.e., z'). This direction was measured with two profile scanners (Sc1, Sc2). The horizontal alignment of the rotation axis with the beam axis was done carefully in order to reduce false asymmetries.⁸ Profiles were measured for “normal” ($\phi_2 = 0^\circ$) and “reversed” ($\phi_2 = 180^\circ$) orientations and the difference of the centroids upon rotation iteratively reduced by horizontal adjustment of POL2. The centroids, measured at the beginning and the end of each run, were found to be normally distributed about the nominal axis with FWHM's of 0.15 mm. This corresponds to an angle spread of 1 mrad FWHM.

D can be expressed in terms of experimentally observed quantities¹¹ as

$$D = A_0^2 \frac{R_0}{\epsilon_0^+ \epsilon_0^-} \frac{(1 - R_1)(1 - R_1 R_2)}{(R_1 - R_0)(R_1 R_2 - R_0)}, \quad (2)$$

where

$$R_1 = (1 + p_0^- A_1)/(1 + p_0^+ A_1) = (1 + \epsilon_1^-)/(1 + \epsilon_1^+)$$

is the intensity ratio in the scattering from T_1 upon spin reversal and $R_0 = p_0^-/p_0^+ = \epsilon_0^-/\epsilon_0^+$ and $R_2 = p_1^-/p_1^+$

$= \epsilon_2^-/\epsilon_2^+$ are the polarization ratios of the incident and scattered beam. The ϵ_i^\pm represent left-right asymmetries, obtained at POL0 ($i=0$), after the scattering ($i=1$), and at POL2 ($i=2$). A_0 , the proton-carbon analyzing power for POL0, was extrapolated from the nearby precise calibration point $A(71.2 \text{ MeV}, 44.0^\circ) = 0.9864 \pm 0.0010$,¹² using the energy dependence given by Ref. 13. This calibration, obtained in a separate experiment with a natural-carbon target for T_1 , exploited a method, which, in contrast to Eq. (2), only involves the ratios R_i .

The ratios R_i are essentially independent of the effective analyzing powers of the polarimeters and rather insensitive to instrumental asymmetries; hence our main concern was the extraction of the POL0 asymmetries ϵ_0^\pm . We used a special technique, which is based on the count rate ratios R^+/R^- and L^+/L^- and exploits the fact that $\partial A_y/\partial \theta = 0$ at 44.0° .^{11,12} While this allowed us to determine ϵ_0^\pm independently for each spin state with little sensitivity to misalignments, contributions due to background and target impurities within the integration limits affect ϵ_0^\pm directly. The background, assumed to be linear, was fitted to the spectra below the ground state and well above any contaminant contribution and average correction factors were extracted. The tail of a small ^{16}O target impurity, monitored continuously with an additional NaI(Tl) detector at 64° , extended into the integration range and a correction $\Delta \epsilon_0^\pm \leq 0.001$ had to be applied. The whole procedure was tested by inserting a graphite target for T_1 at regular intervals at $\theta^{\text{lab}} = 32^\circ, 36^\circ, 40^\circ, 44^\circ, 52^\circ, 60^\circ$. Using A_0 as given above, we obtained $D = 1.0001 \pm 0.0012$, in excellent agreement with the expectation value $D \equiv 1$ for spin- $\frac{1}{2}$ from spin-0 scattering. The distribution of the individual values was found to be completely statistical ($\chi^2 = 24.3$ for 26 data points) and showed no indication of an angle dependence. The same background reduction procedure was then applied to the actual ^{13}C measurements performed under identical background conditions.

R_1 was obtained from the left-right sum of the POL2 side detectors and R_2 by taking the geometric mean of the count rates for normal and reversed orientation.⁸ The count rates were normalized to the FC integrated charge and corrected for dead-time effects.

Data were taken in four run times. At each angle about five run pairs were recorded, where a pair consisted of two measurements, taken with normal and reversed orientation. The beam polarization was flipped every 10 s between typically $p_0^+ = 0.87$ and $p_0^- = -0.89$. The beam intensity varied between 0.8 and 2.4 μA .

Two corrections to the raw data were applied: (1) The finite geometry correction (≤ 0.003) was obtained from Monte Carlo calculations, based on existing analyzing-power and cross-section data.^{10,13} (2) The correction for the ^{12}C impurity of the targets (≤ 0.003) was derived from a determination of the ^{12}C contents by mass spec-

trometry ($11\% \pm 2\%$). We saw no indication of other impurities based on periodic measurements of the energy spectrum of the scattered beam, obtained by scanning the magnetic field of the dipole.

Apart from the statistical uncertainty ($0.002 \leq \Delta_{\text{stat}} \leq 0.004$) various systematic errors contribute to the final errors. Angle-dependent contributions due to non-proper spin flip⁸ arise from imperfect alignment of the POL2 rotation axis with the axis of the scattered beam ($\Delta_{\text{npf}} \leq 0.001$). The error estimate was based on the variation of the scanner centroids and on an estimate of the alignment uncertainties for both side detectors. Other systematic contributions may arise due to correlations between the polarization and the energy of the scattered beam with its position and angle at the POL2 targets. Upper limits ($\Delta_{\text{corr}} \leq 0.002$) were calculated assuming a linear dependence of the polarization and energy on the horizontal phase-space coordinates at the AT's. Measurements of the ratio R_1 as a function of the scanner positions at an angle where $A_1(\theta_1)$ shows a steep gradient are consistent with these assumptions.

The uncertainties due to various other effects (POL2 spectra integration, corrections for finite geometry, ^{12}C and dead time, energy averaging in T_1 , and energy differences between run times) were estimated to be well below 0.001, respectively. An angle-independent contribution (0.0015) was due to the POL0 integration problem discussed before.

Figure 2 shows the final results. The errors represent the root square sum of the statistical and all systematic errors. The normalization uncertainty due to the error in A_0 is not included. Since several systematic errors are common to both experiments, the resulting uncertainty for D is 0.0012.

Two different approaches have been used to analyze the data: In the first one D was fitted with an optical-model (OM) potential which, in addition to the conven-

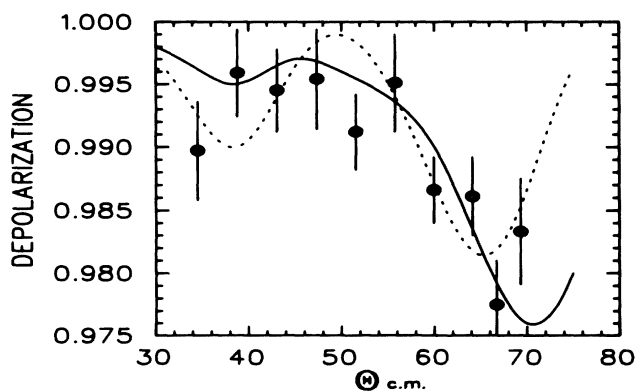


FIG. 2. The depolarization parameter D for \bar{p} - ^{13}C elastic scattering at 72 MeV. The solid curve represents a microscopic prediction. The dashed curve represents the best fit with the phenomenological OM potential mentioned in the text.

tional part, included real spin-spin potentials of spherical (V_{ss}) and tensor type (V_{st}).¹ The small spin-spin potentials were treated as perturbations.^{1,14} The parameters without spin-spin potentials were determined by a fit to $d\sigma/d\Omega$, σ_R , and A_y ,¹⁰ which are insensitive to spin-spin effects. The geometry for both spin-spin potentials was chosen to be the same. We found that D can be reproduced using a real spherical spin-spin potential alone. Volume-type form factors fit the data only for unrealistic values of the diffuseness parameter ($a_{\text{ss}}=0.1$), whereas for surface type good fits were achieved with normal geometry parameters. This finding supports the naive interpretation of spin-spin effects as due to an interaction with the valence nucleons. The best fit ($V_{\text{ss}}=0.7$ MeV, $r_{\text{ss}}=1.65$ fm, $a_{\text{ss}}=0.50$ fm) is represented by the dashed curve in Fig. 2. The uncertainty of V_{ss} (0.1 MeV) includes the usual statistical error of the fit as well as an estimate of the uncertainties of the conventional OM parameters and of the effect of possible correlations between different parameters. It should be pointed out, however, that with inclusion of a tensor-type potential, V_{ss} changes drastically even for very small V_{st} . For instance, the combination $V_{\text{ss}}=0.5$ MeV, $V_{\text{st}}=0.05$ MeV, $r_{\text{ss}}=r_{\text{st}}=1.65$ fm, and $a_{\text{ss}}=a_{\text{st}}=0.50$ fm fits the data equally well.

In the microscopic approach the nucleon-nucleus potential was calculated by averaging an effective interaction between the projectile and a target nucleon over the distribution of the nucleons in the target. The effective interaction was based on the Paris NN potential¹⁵ and the local-density approximation. The wave functions used¹⁶ reproduce other valence-nucleon-dependent observables such as the magnetic moment and the transverse form factor for elastic electron scattering.¹⁷ The solid line in Fig. 2 shows that this calculation is in good agreement with our data.

In conclusion, we have reported the first significant measurement of the depolarization parameter D for elastic proton scattering from a spin- $\frac{1}{2}$ nucleus at an energy where compound-nucleus contributions are negligible. The data reveal a deviation from unity of 0.02 around the second diffraction minimum, which was determined with an overall accuracy of 0.003–0.004 per data point. Our data represent unambiguous evidence for spin-spin effects in nucleon-nucleus scattering and are well described by a microscopic calculation based on the Paris potential. An OM approach, which includes a real spherical spin-spin potential with surface form factor, also reproduces the data, yielding $V_{\text{ss}}=0.7 \pm 0.1$ MeV for the strength of the potential.

This work was supported in part by Bundesministerium für Forschung und Technologie and the Swiss National Foundation.

(a)Present address: TRIUMF, Vancouver, Canada.

¹H. S. Sherif, in *Proceedings of the Fourth International*

Symposium on Polarization Phenomena in Nuclear Reactions, Zürich, 1975, edited by W. Grüebler and V. König (Birkhäuser, Basel, 1976), p. 189.

²C. R. Gould, D. G. Haase, L. W. Seagondollar, J. P. Soderstrum, K. E. Nash, M. B. Schneider, and N. R. Roberson, *Phys. Rev. Lett.* **57**, 2371 (1986); C. R. Gould, N. R. Roberson, and W. J. Thompson, *Phys. Rev. Lett.* **60**, 2335 (1988).

³S. F. Mughabghab, *Phys. Rev. Lett.* **54**, 986 (1985); **56**, 399 (1986).

⁴G. Roy, H. S. Sherif, E. D. Cooper, L. G. Greeniaus, G. A. Moss, J. Soukoup, G. M. Stinson, R. Abegg, D. P. Gurd, D. A. Hutcheon, R. Liljestrand, and C. A. Miller, *Nucl. Phys.* **A442**, 686 (1985).

⁵V. Hnizdo and K. W. Kemper, *Phys. Rev. Lett.* **59**, 1892 (1987).

⁶S. Raman and J. E. Lynn, *Phys. Rev. Lett.* **56**, 398 (1986).

⁷N. Nakamura, H. Sakaguchi, H. Sakamoto, H. Ogawa, O. Cynshi, S. Kobayashi, S. Kato, N. Matsuoka, K. Hatanaka, and T. Noro, *Nucl. Instrum. Methods Phys. Res.* **212**, 173 (1983).

⁸G. G. Ohlsen, in *Proceedings of the Fourth International Symposium on Polarization Phenomena in Nuclear Reactions, Zürich, 1975*, edited by W. Grüebler and V. König

(Birkhäuser, Basel, 1976), p. 287.

⁹B. v. Przewoski, P. D. Eversheim, F. Hinterberger, U. Lahr, J. Campbell, J. Götz, M. Hammans, R. Henneck, G. Masson, I. Sick, and W. Bauhoff (to be published).

¹⁰B. v. Przewoski, P. D. Eversheim, F. Hinterberger, L. Doberitz, J. Campbell, M. Hammans, R. Henneck, W. Lorenzon, M. A. Pickar, and I. Sick, *Nucl. Phys.* **A496**, 15 (1989).

¹¹F. Hinterberger, U. Lahr, B. v. Przewoski, and R. Henneck, *Nucl. Instrum. Methods Phys. Res., Sect. A* **284**, 523 (1989).

¹²P. D. Eversheim, F. Hinterberger, U. Lahr, B. v. Przewoski, J. Campbell, J. Götz, M. Hammans, R. Henneck, G. Masson, and I. Sick (to be published).

¹³M. Ieiri, H. Sakaguchi, M. Nakamura, H. Sakamoto, H. Ogawa, M. Yosoi, T. Ichihara, N. Ishiki, Y. Takeuchi, H. Togawa, T. Tsutsumi, S. Hirata, T. Nakano, and S. Kobayashi, *Nucl. Instrum. Methods Phys. Res., Sect. A* **257**, 253 (1987).

¹⁴H. S. Sherif, code RELSPIN, University of Alberta, 1986.

¹⁵M. Lacombe, B. Loiseau, J. M. Richard, R. Vinh Mau, J. Cote, P. Pires, and R. de Turreil, *Phys. Rev. C* **21**, 861 (1980).

¹⁶S. Cohen and D. Kurath, *Nucl. Phys.* **73**, 1 (1965).

¹⁷T. W. Donnelly and I. Sick, *Rev. Mod. Phys.* **56**, 461 (1984).